

STRESS-STRAIN STUDY NEAR CRACKS IN RUBBER MODELS BY NONLINEAR PHOTOELASTICITY

G.N. Albaut, N.V. Kharinova

Novosibirsk State University of Architecture and Civil Engineering (Sibstrin)
630008, Novosibirsk, Russia

ABSTRACT

Problems of elastic nonlinear deformation were studied in the conditions of large displacement. Experimental works were executed by a method of nonlinear photoelasticity in course of investigating plane models by polarizative light. Stresses, strains and coefficients of their concentration in the plates having central crack-cuts including inclined ones were determined. All results were obtained in two curvilinear systems of coordinates (Euler and Lagrange).

1 INTRODUCTION

Research problems of the large elastic strains take place in pneumoinflatable envelopes and rubbertechnical products at designing and exploitation stages. Sources of stress concentration and defects as cracks are especially dangerous. Because of the complexity of the mathematical calculations for similar tasks practically there are no reliable and available engineering methods of estimation. Experimental researches also become complicated owing to the necessity of considering changes of the sizes of elements under deformation. The main thesis and dependences of nonlinear elastic theory given in works of professor Chernykh [1, 2] were used to describe of nonlinear deformation processes in rubber specimens. We checked some of his ideas and analytical decisions of nonlinear problems by experiment.

All models were made from Russian polyurethane (mark SKU-6), which had height optical sensitive and elastic properties. Theoretic bases of nonlinear photoelasticity method are offered in works of Albaut [3, 4, 5], where main optical dependences, methods of stress and strain division and others are given. The processing of experimental data in this work was held by this methodic.

At the large strains when it is impossible to neglect changes of the element sizes, the equations of the mechanics obtained at small strains cease to be fair and relative strains and shifts (the Koshiy measure of strains) any more are not tensor values and becomes inconvenient for practical use. At research of nonlinear problems two curvilinear systems of coordinates (Euler and Lagrange) are used, stresses and strains in which are described by pair connected tensors. In system of coordinates Lagrange is tensor of conditional stresses σ^L and tensor Green's strains, and in Euler coordinates these are the tensors of true stresses of Koshiy σ and strains of Almanzy-Hammel.

The Lagrange system of coordinates is more expedient for using at the theoretical decision of problems when the initial sizes of a body and its kind before deformation are known, and the Euler system of coordinates is used at experimental researches since in this case there is a deformed kind of researched samples.

Investigations were sponsored by Russian Fund of Fundamental Investigations (Project №02-01-00222).

2 CONCENTRATION OF STRESSES AND STRAINS AT THE TOP OF INCLINED CRACKS

Graphic dependences showing changes of concentration coefficients of true stress K_σ (Euler coordinates), conditional stress K_σ^L (Lagrange coordinates) as well as strains K_ε (relative lengthenings) were drawn on the basis of experimental data depending on the values of nominal longitudinal strains (ε_i) or stretches (λ_i). Strips with an inclined crack-cut, Figure 1, were subject to

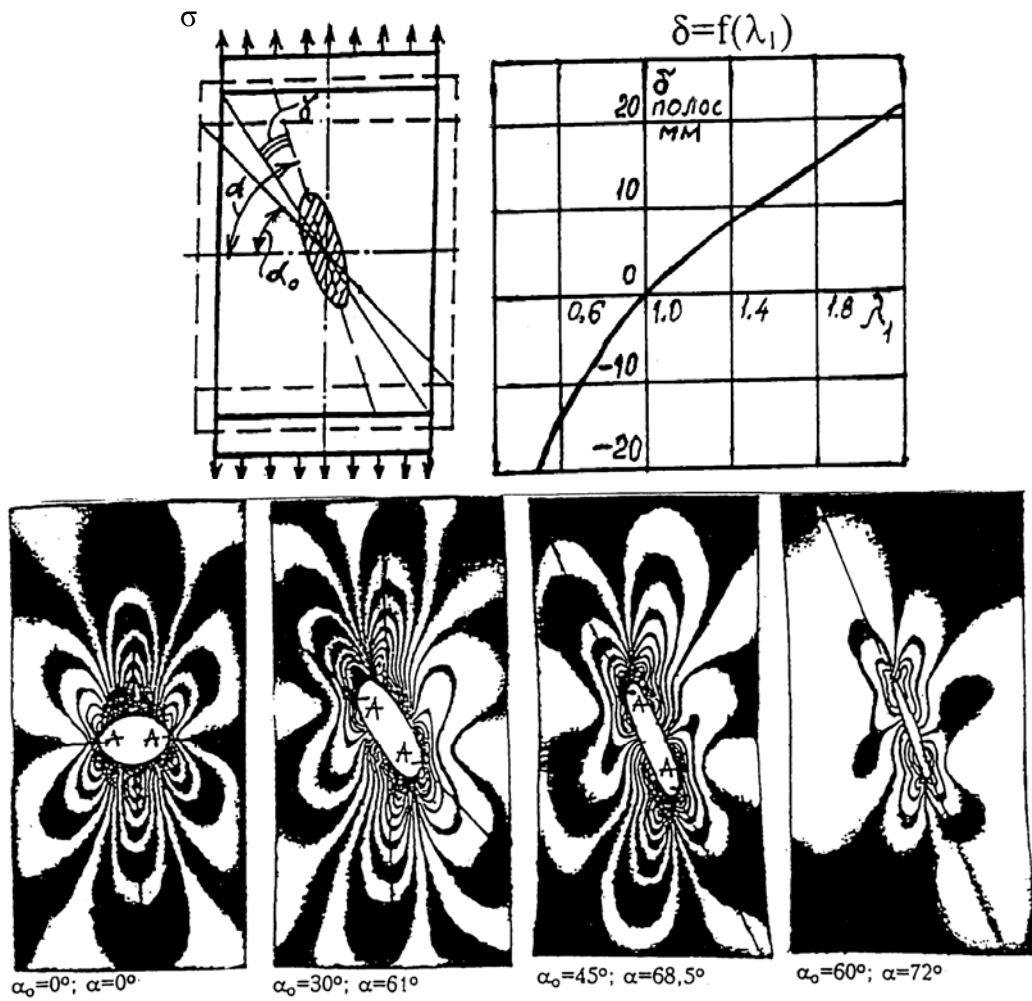


Figure 1: Scheme of the sample and interference fringe patterns.

tension. The initial angles of an inclination of a crack with a horizontal axis were $\alpha_0 = 0^\circ, 30^\circ, 45^\circ, 60^\circ$.

Concentration coefficients of stresses K_σ , K_σ^L and strains K_ε were calculated by dependences:

$$K_\sigma = \frac{\sigma_{\max}}{\sigma_0}; \quad K_\varepsilon = \frac{\lambda_{\max} - 1}{\lambda_0 - 1}; \quad K_\sigma^L = \frac{\sigma_{\max}^L}{\sigma_H^L} = K_\sigma \frac{A_{\max}}{A_H}. \quad (1)$$

Here σ_{\max} and λ_{\max} are the maximum true stress and strain near crack top, and σ_0 and λ_0 – nominal ones at a distance. A_{\max} and A_H – the corresponding individual areas of cross section in Euler coordinates in a zone of an axial tension, i.e. $A_{\max} = 1/\lambda_{\max}$; $A_H = 1/\lambda_H$. These data were obtained with the help of interference fringe patterns and test diagram $\delta = f(\lambda_1)$, Figure 1.

The analysis of fringe patterns given in Figure 1 shows that under loading all crack-cuts open and turn into ellipses. The largest disclosing of a crack was observed when $\alpha_0 = 0^\circ$, decreasing in a sequence $\alpha_0 = 30^\circ, 45^\circ, 60^\circ$ under the same loading. The tops of ellipse to which the crack was transformed didn't coincide with the tops of the initial crack-cut (point A on photos) and moved aside to the axis of tensioning.

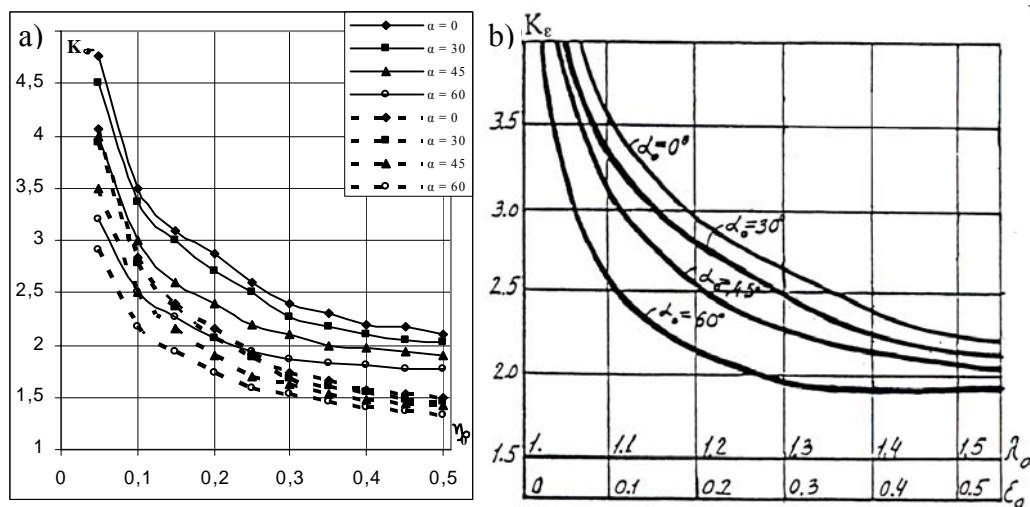


Figure 2: Graphics of the change of concentration coefficients of the true K_{σ} , conditional K_{σ}^L stresses and strains K_{ϵ} .

Graphic dependences of the change of concentration coefficients of true stresses K_{σ} and nominal strains K_{ϵ} at tops of inclined cracks at the beginning were drawn depending on the values of nominal deformations λ_0 or ϵ_0 (relative lengthenings) with the use of formulas (1). They were represented by continuous lines for four initial angles of crack inclination shown above in Figure 2. The corresponding diagrams of change K_{σ}^L were shown by dotted lines in Figure 2a.

It is possible to note if we compare graphs K_{σ} , K_{σ}^L or K_{ϵ} for different samples that during tensioning of a strip with a horizontal crack had the biggest values of concentration coefficients and the coefficients of concentration decrease at the increase of angles of cracks inclination.

In all graphs, Figure 2, as the nominal strains increase concentration coefficients of stresses decrease along a smooth curve approaching to some asymptote values. For example, for a curve with $\alpha_0=0^0$ the value of asymptote is $K_{\sigma}=2$ (Euler coordinates), and $K_{\sigma}^L=1.45$. For other angles of inclination its value was a little bit less.

In linear problems it is $K_{\sigma}=3$ for a round hole. One can see the same asymptote in the present problem when geometry changes, but K_{σ} is much less in rubber.

Destruction of models with inclined cracks in experiments was from initial tops of a crack along a horizontal line, perpendicular to the loading.

3 DETERMINATION OF PREFRACTION STRESSES

The results of quantitative research of stresses were given under tensioning of plane plates of various thickness with the central crack. Models were made as crosswise plates according to the scheme, Figure 3. The crack was made with a sharp edge. The initial processing of experimental data was carried out in Euler coordinates with the use of the true stresses relative to the deformed area (σ_1 and σ_2 - in a plane, and σ_3 - along thickness). Strains were measured with the help of stretches with the principal components $\lambda_i=l_i/l_0$ (l_0 and l_i - the size of an element before and after deformation; λ_1 and λ_2 - in a plane, and λ_3 - along thickness). As a result of polarization-optical experiment a picture of interference fringe patterns in the models actually representing the fields of differences of the main relative strengths $\lambda_3(\sigma_1-\sigma_2)$ determined by the formula (2), and fields isoclin Θ - angles of an inclination of the principal stresses were obtained. The differences of

normal and tangents strengths in a plane of model $\lambda_3(\sigma_x - \sigma_y)$ and $\lambda_3\tau_{xy}$ on (3) were obtained in accordance with the experimental data.

$$\lambda_3(\sigma_1 - \sigma_2) = \frac{\sigma_0^{1,0} n}{h_0}; \quad (2)$$

$$\lambda_3(\sigma_x - \sigma_y) = \lambda_3(\sigma_1 - \sigma_2) \cos 2\Theta; \quad \lambda_3\tau_{xy} = \lambda_3(\sigma_1 - \sigma_2) \sin 2\Theta. \quad (3)$$

Here h_0 is the initial thickness of the sample.

Full division of stresses and strains was carried out by a method of numerical integration of one of the differential equations of balance (4) using a condition of stability of the volume (5) and physical equations of connection (6) obtained on the basis of Bartenev-Khazanovitch elastic potential, Akhmetzyanov [4]:

$$\frac{\partial(\lambda_3\sigma_x)}{\partial x} + \frac{\partial(\lambda_3\tau_{xy})}{\partial y} = 0; \quad \frac{\partial(\lambda_3\tau_{yx})}{\partial x} + \frac{\partial(\lambda_3\sigma_y)}{\partial y} = 0; \quad (4)$$

$$\lambda_1\lambda_2\lambda_3 = 1; \quad (5)$$

$$\sigma_1 = A(\lambda_1 - \lambda_3); \quad \sigma_2 = A(\lambda_2 - \lambda_3). \quad (6)$$

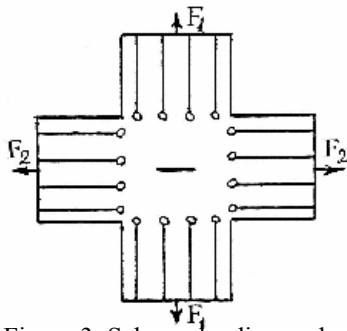


Figure 3: Scheme loading under two-dimensional tension.

A - constant of Bartenev-Khazanovitch elastic potential.

Figure 4 gives pictures of interference fringe patterns in plate under uniaxial tension of a thin plate with the sharp crack which turned during deformation into a circle was investigated; nominal deformations came to 100%. The epures of the principal true stresses σ_1 and σ_2 (Euler coordinates) which then were recalculated in conditional stresses, related to the non deformed area σL_1 and σL_2 (Lagrange coordinates) were shown in Figure 4 in the given vertical and horizontal sections. As one can see, conditional stresses σL_1 are a little bit less than true σ_1 while σL_2 practically coincide with σ_2 , and sometimes they are even larger. While analyzing the graphs of stresses, it is possible to notice some of their features characteristic for all

samples. Stress σ_2 is of great importance for revealing the mechanism of destruction. They are two-signed, have wavy character in the vertical section, Figure 4, and this provides a possibility of balance of strengths in each section by the sum of projections of all forces on a horizontal axis. Generally, tension stresses σ_1 increase near crack tops. However, the fact of the shift of maximum σ_1 (section 1-1) from the tops of a crack deep into a sample that seems to be an unusual phenomenon. The value σ_1 at the top reduces to 20% and for σL_1 to 13%. A similar displacement of a maximum σ_1 from the source of the concentration inside the model obtained by calculation methods was mentioned in the monograph "Experimental Techniques in fracture Mechanics" edited by A.Kobajasi [6]. But the level of deformation and displacement was less than in the present work.

It is possible to note one more paradoxical phenomenon while analyzing the interference fringe patterns: the displacement of the maximum value of contour stress from geometrical sources of concentration to some distance along the contour of holes, Figure 4.

Crack-cut tops become blunt, the geometry of concentrators smoothes in the zone of large deformations during the process of element's deforming. It is especially evident from the picture of transformations of sharp cracks in rubber plates, which turn into ellipses under deformation, in this case sharp tops of cracks are so blunt, that they can't be seen in pictures, Figure 4.

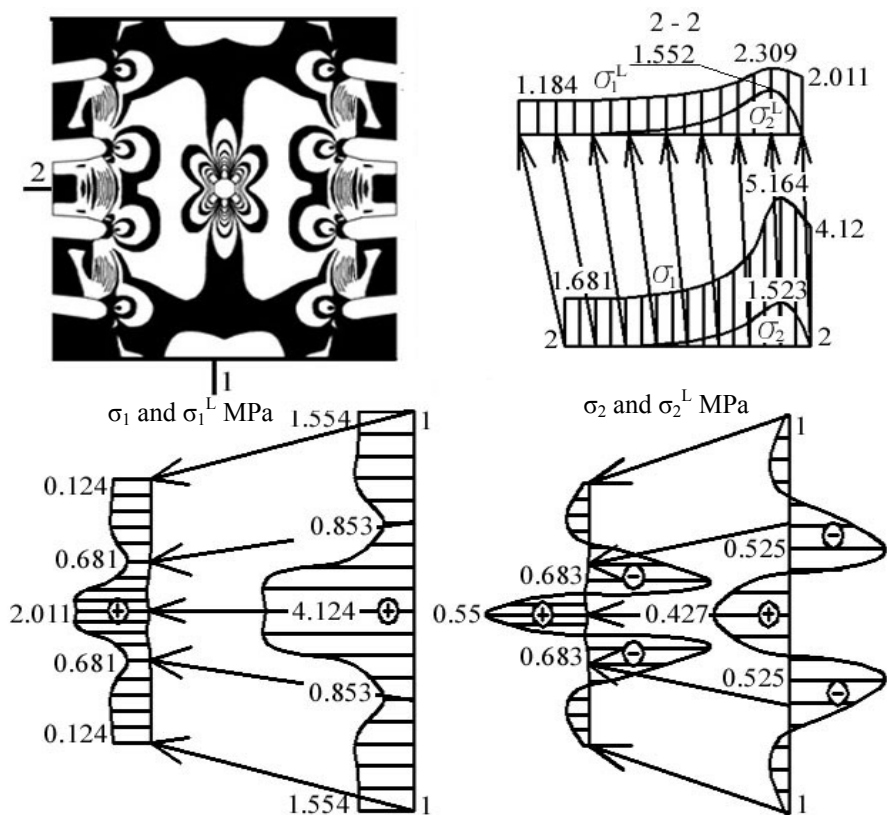


Figure 4: The picture of fringe patterns in the model and epures of principle true σ and conditional σ^L stresses.

REFERENCES

1. Chernykh K.F. Introduction in physical and geometrical crack theory, M: Nauka, P. 287, 1996, (in Russia).
2. Chernykh K.F. Nonlinear theory of anisotropic elasticity. USA, N.T.: Begell Publishing House, P. 342, 1998.
3. Albaut G.N., Baryshnikov V.N. Stress-strain investigation near cracks in rubber specimens by photoelastic method, Photomechanics'95, Proc. SPIE, Vol. 2791, P. 50-55, 1996.
4. Akhmetzyanov M., Albaut G. Study of large plastic strains and fracture in metal elements by photoelastic coating method, International Journal of Fracture, Kluwer Academic Publishers, 128(1), P. 223-231, July, 2004 – August, 2004.
5. Albaut G.N., Baryshnikov V.N. Investigation of mechanics of fracture problems by non-linear photoelastic method, Proc. SPIE, Vol. 2791, P. 56–67, 1996.
6. Experimental Techniques in fracture Mechanics, V.1, 2, Eg. by A.S.Kobayashi, publ. jointly by the Iowa State Univ. Press and Soc. For Exper. Stress Analysis, 1973.